IOP Publishing Journal of Physics G: Nuclear and Particle Physics
J. Phys. G: Nucl. Part. Phys. **50** (2023) 065201 (14pp) https://doi.org/10.1088/1361-6471/acc751

Low-energy solar neutrino detection utilizing advanced germanium detectors

S Bhattarai, D-M Mei* and M S Raut

University of South Dakota, Vermillion, SD, 57069, United States of America

E-mail: dongming.mei@usd.edu

Received 14 January 2023, revised 20 March 2023
Accepted for publication 24 March 2023
Published 17 April 2023

Abstract

We explore the possibility to use advanced germanium (Ge) detectors as a low-energy solar neutrino observatory by means of neutrino-nucleus elastic scattering. A Ge detector utilizing internal charge amplification for the charge carriers created by the ionization of impurities is a novel technology with experimental sensitivity for detecting low-energy solar neutrinos. Ge internal charge amplification (GeICA) detectors will amplify the charge carriers induced by neutrino interacting with Ge atoms through the emission of phonons. It is those phonons that will create charge carriers through the ionization of impurities to achieve an extremely low energy threshold of ∼0.01 eV. We demonstrate the phonon absorption, excitation, and ionization probability of impurities in a Ge detector with impurity levels of 3×10^{10} cm^{-3}, 9×10^{10} cm^{-3}, and 2×10^{11} cm^{-3}. We present the sensitivity of such a Ge experiment for detecting solar neutrinos in the low-energy region. We show that, if GeICA technology becomes available, then a new opportunity arises to observe *pp* and ^{7}Be solar neutrinos. Such a novel detector with only 1 kg of high-purity Ge will give ∼10 events per year for *pp* neutrinos and ∼5 events per year for ^{7}Be neutrinos with a detection energy threshold of 0.01 eV.

Keywords: solar neutrinos, germanium detector, phonons

(Some figures may appear in colour only in the online journal)

1. Introduction

Solar neutrinos are produced in the core of the Sun through nuclear fusion reactions. The study of solar neutrinos provides information about the fundamental properties of neutrinos and allows us to understand how the Sun works. There are various nuclear fusion reactions occurring in the Sun that produce solar neutrinos of different fluxes and their spectra [1]. The

* Author to whom correspondence should be addressed.

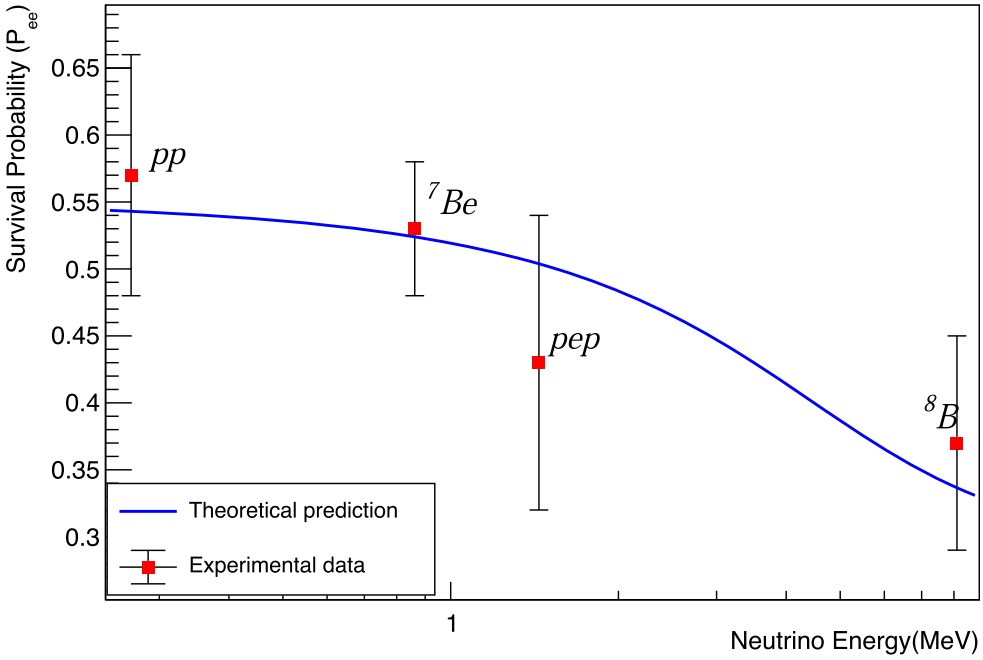

Figure 1. Survival probability of solar neutrinos from *pp* chain [15].

solar neutrinos emitted in several steps of the proton–proton cycle are *pp*, *pep*, ^{7}Be, ^{8}B and *hep* neutrinos. On the other hand, solar neutrinos produced in the carbon–nitrogen–oxygen cycle are mostly ^{13}N, ^{15}O and ^{17}F neutrinos [2, 3]. The energy range of these neutrinos varies from a few keV to a few MeV. Detecting these neutrinos by placing a detector in an underground laboratory has always been a challenge. A suitable energy threshold for detecting each of these neutrinos is difficult to achieve. Numerous collaborations have used different detector materials and techniques to study solar neutrinos. Homestake [4], Super-Kamaiokande [5, 6], SNO [7, 8], BOREXINO [9, 10], GALLEX/GNO [11], SAGE [12], LENS [13], are some of the experiments that studied solar neutrinos with the detection energy threshold greater than 233 keV. By detecting the flux of neutrinos from the ^{8}B reaction in the Sun, SNO was able to completely demonstrate neutrino flavor transition using charge current (cc) and neutral (nc) current reactions [7]. The comparison of reaction rate between cc and nc reactions help in the measurement of total electron neutrino (ν_e) flux and the total flux independent of the flavor (ν_e, ν_τ, ν_μ). A strong suppression of electron neutrinos was observed relative to that expected in the standard solar model (SSM) [14]. This showed that solar neutrinos are changing into other neutrinos by neutrino flavor transition. The most accurate measurement of neutrino survival probability to date is observed by Borexino [15]. They used elastic neutrino-electron scattering to experimentally calculate the values of survival probability [15] for four-electron neutrino components of the *pp* chain which is shown in figure 1. There is a certain amount of difference between the theoretical [16–19] and the experimental values as depicted in figure 1.

Over 99 percent of the total solar neutrinos produced from *pp* cycles are believed to be *pp* neutrinos [1]. They exhibit a continuous spectrum with an end-point energy of 423 keV, which makes it difficult to be detected using liquid scintillation detectors. This is because the energy deposited through elastic neutrino-nucleus scattering falls below the detection

threshold and the energy induced by elastic neutrino-electron scattering is often contaminated by backgrounds. Therefore, the measured event rate from *pp* neutrinos can be largely uncertain as shown by Borexino [9].

For a solid-state detector, such as a Ge detector, both elastic neutrino-nucleus scattering and elastic neutrino-electron scattering can be detected. However, since the detectors are much smaller in size compared to liquid scintillation detectors, the energy deposited through elastic neutrino-electron scattering is often immersed in backgrounds. Nevertheless, the event rate grows exponentially as a function of nuclear recoil energy through elastic scattering off the nucleus. It is expected that the event rate will significantly surpass the background in the low energy range of nuclear recoils. This is because the expected nuclear recoil events (signal) grow exponentially while electric recoil events (background) remain flat in the region of interest. Thus, elastic neutrino-nucleus scattering represents a viable tool to measure *pp* neutrinos in a Ge detector. The maximum nuclear recoil energy produced by *pp* neutrinos via elastic neutrino-nucleus scattering in a Ge detector is $\sim$5.2 eV. Hence, to detect the *pp* solar neutrinos, an extremely low-energy threshold detector is needed. CDMS [20], SuperCDMS [21] and EDELWEISS [22] have demonstrated that the energy threshold of $\sim$50 to $\sim$100 eV can be achieved in Ge detectors through the detection of phonons. In 2018, SuperCDMS reported a 3 eV phonon energy resolution with a 0.93 gram Si detector when biased at 100 V [23].

Nevertheless, nuclear recoils induced by *pp* neutrinos require detectors of a threshold lower than 1 eV to have meaningful statistics. Therefore, because the current state-of-the-art Ge detectors cannot detect the *pp* neutrinos through elastic neutrino-nucleus scattering, a new type of detector is required. A Ge internal charge amplification (GeICA) detector, which amplifies the charge carriers created by the ionization of impurities, is a novel technology with experimental sensitivity for detecting the low-energy solar neutrinos [24, 25]. With an extremely low-energy threshold ($\sim$0.01 eV), GeICA detectors can measure the *pp* neutrinos flux through coherent elastic neutrino-nucleus scattering with good statistics and hence the current uncertainty in neutrino survival probability (figure 1) can be decreased. In this paper, we describe the GeICA detector technology for achieving sensitivity in detecting low-energy *pp* neutrinos. GeICA will amplify the charge carriers induced by *pp* neutrinos interacting with Ge atoms through the emission of phonons [24]. It is those phonons that will create charge carriers through the ionization of impurities to achieve an extremely low energy threshold of $\sim$0.01 eV. Detection of low-energy solar neutrinos is an important area of research because these neutrinos can provide valuable information about the nuclear reactions occurring in the Sun, which ultimately drive the Sun's energy production. The use of a Ge internal charge amplification detector for this purpose is novel because it offers several advantages over other types of detectors.

One advantage of using a Ge internal charge amplification detector is that it is capable of detecting low-energy neutrinos with high efficiency. This is because the Ge detector is able to amplify the charge produced by the interaction of a neutrino with the detector material, making it easier to detect even very low-energy neutrinos.

Another advantage of using a Ge internal charge amplification detector is that it has a low background noise level, which allows for the detection of weak signals produced by low-energy neutrinos. This is particularly important for detecting solar neutrinos, which have relatively low energy compared to other types of neutrinos.

Finally, the use of a Ge internal charge amplification detector is novel because it allows for the measurement of the energy of the detected neutrinos with high precision. This is important because the energy of the solar neutrinos can provide valuable information about the nuclear reactions occurring in the Sun.

Overall, the use of a Ge internal charge amplification detector for the detection of low-energy solar neutrinos is a novel and effective approach that offers several advantages over other types of detectors [25].

Coherent elastic neutrino-nucleus scattering has not been used for detecting *pp* neutrinos because of the low amount of energy transferred to a nucleus during the interaction. However, utilizing internal charge amplification, the charge carriers created by phonon excitation can be used to detect *pp* neutrinos because of the extremely low energy threshold of the detector [26]. In addition, the size of the detector can be dramatically reduced. The event rate from coherent elastic neutrino-nucleus scattering is much higher than that of elastic neutrino-electron scattering. The differential neutrino-nucleus cross section $\mathrm{d}\sigma_{\mathrm{CNS}}(E_\nu, E_{\mathrm{NR}})/\mathrm{d}E$ for a neutrino of energy E_ν (eV) is given by

$$\frac{\mathrm{d}\sigma_{\mathrm{CNS}}(E_\nu, E_{\mathrm{NR}})}{\mathrm{d}E_{\mathrm{NR}}} = \frac{{G_{\mathrm{F}}}^2}{4\pi} {Q_w}^2 m_N \left(1 - \frac{m_N E_{\mathrm{NR}}}{2{E_\nu}^2}\right) F^2(T_R), \tag{1}$$

where E_{NR} is nuclear recoil energy, m_N is the mass of the target nucleus, G_{F} is the Fermi Coupling constant, $Q_w = N - (1 - 4\sin^2\theta_w)Z$ where N the number of neutrons and Z is the number of protons and θ_w the weak mixing angle. Here, the value of the form factor $F(T_R)$ is equal to 1 [27]. Likewise, the differential event rate for a detector of mass M and exposure time T is given by

$$\frac{\mathrm{d}E}{\mathrm{d}E_{\mathrm{NR}}} = N_T \times M \times T \times \frac{\mathrm{d}\sigma_{\mathrm{CNS}}(E_\nu, E_{\mathrm{NR}})}{\mathrm{d}E_{\mathrm{RN}}} \times \frac{\mathrm{d}N_\nu}{\mathrm{d}E_\nu}, \tag{2}$$

where N_T is the number of target nuclei per unit mass and $\frac{\mathrm{d}N_\nu}{\mathrm{d}E_\nu}$ is the differential neutrino flux. Figure 2 shows the expected event rate as a function of nuclear recoil energy induced by solar neutrinos in a Ge detector. Through coherent elastic neutrino-nucleus scattering, we can detect *pp* neutrinos in different flavors (ν_e, ν_τ, ν_μ) without considering the neutrino oscillation. This leads to the determination of total neutrino flux in the detector. Similar to the SNO experiment, which determined the total $^{8\mathrm{B}}$ neutrino flux and hence proved the neutrino flavor transition, measuring the total *pp* neutrino flux will verify the SSM and the neutrino flavor transition at lower neutrino energy when combined with the global measurements for the solar neutrino survival probability, as shown in figure 1. Table 1 shows the maximum recoil energy induced by solar neutrinos and the total event rate integrated for solar neutrinos in a Ge detector with a mass of 1 kg.

Below, we demonstrate how *pp* neutrinos can be measured more accurately with the proposed Ge detector that uses phonons generated by neutrinos via coherent neutrino-nucleus elastic scattering to ionize impurities.

2. The working principle of the proposed detector

Starostin *et al* [26] have proposed a detector that can be used to amplify the signal generated by the *pp* solar neutrinos. It is assumed to be made from a 1.0 kg HPGe crystal. The net impurity concentration in the detector will be $(1–3) \times 10^{10}$ cm^{-3}. It will be a multi-strip planar Ge detector having a dimension of 9 cm × 7 cm × 3 cm with 15 anode strips fabricated using the photo-mask method each of width 20 μm. The fiducial volume of the detector will be about 190 cm^3 [24, 26]. The detector concept and its working principle were discussed in detail in our earlier publication [24]. The main conclusions are:

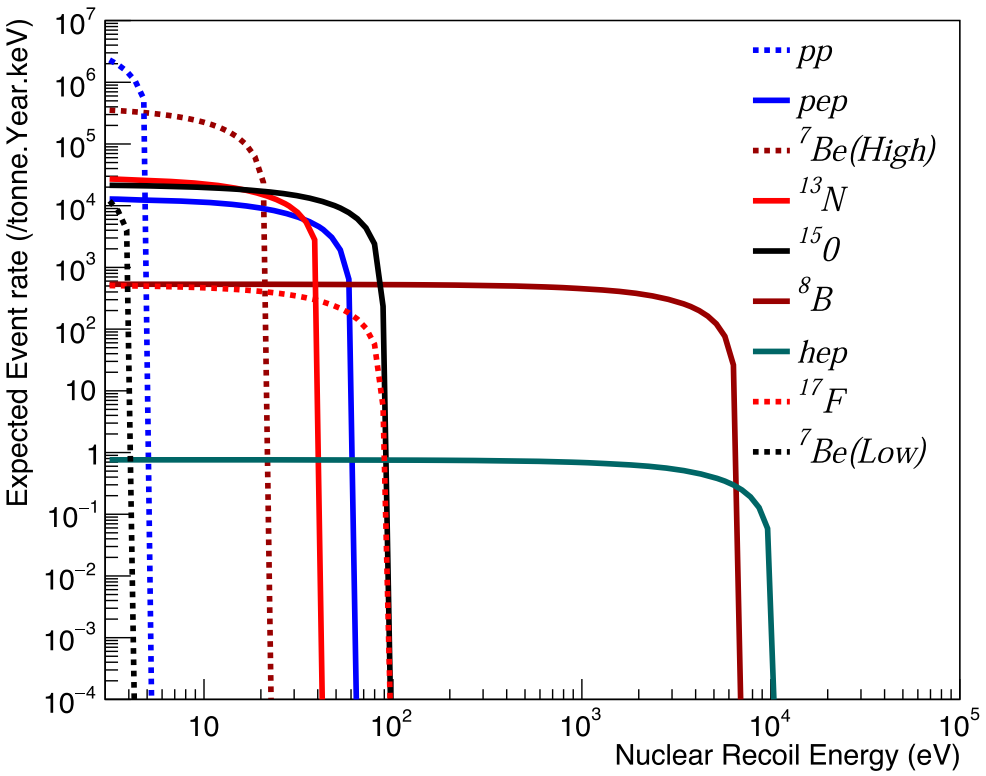

Figure 2. The expected event rate versus nuclear recoil energy produced by solar neutrinos in a Ge target. The label of *y*-axis is the event rate in a Ge detector for different solar neutrinos in the unit of tonne^{-1} year^{-1} keV^{-1}. This gives the event rate produced by solar neutrinos (the flux is in the unit of cm^{-3} sec^{-1}.keV^{-1}) in a Ge detector corresponding to the nuclear recoil energy (in the level of keV) induced by solar neutrinos interacting with Ge nuclei. Here, keV stands for kilo electron volts.

(i) After purifying Ge ingots to a level of $\sim 10^{11}$ cm^{-3} by zone refining [28], a single crystal can be grown at the University of South Dakota (USD) through the Czochralski method [29]; during the crystal growth process, impurities can be further removed from the grown crystal down to a level of $\sim 10^{10}$ cm^{-3} or below [30].

(ii) It has been found that the remaining impurities are mainly aluminum (Al), phosphorous (P), boron (B), and gallium (Ga) in the USD-grown crystals [29]; the ionization energies of these impurities in Ge are in a level of $\sim$0.01 eV, which is less than the longitudinal acoustic (LA) phonon (0.04 eV) and the transverse (TA) phonon (0.026 eV) generated by neutrinos via coherent neutrino-nucleus elastic scattering [24, 31]; hence the phonons can certainly excite or ionize these impurities to produce charge carriers.

(iii) These charge carriers would then be drifted towards the electrical contacts. During the drifting process, these charge carriers would be accelerated by a high electric field to generate more charge carriers and hence, amplify the charge by a factor of $\sim$100 to $\sim$1000, depending on the applied electric field.

(iv) The absorption probability P of phonons in a given Ge detector can be estimated as

$$P = 1 - \exp(-d/\lambda), \tag{3}$$

where d is the average distance diffused before an anharmonic decay and $\lambda = \frac{1}{\sigma \times N_A}$ is the mean free path of phonons with N_A being the net impurity level in a given p-type detector and σ is the cross section of phonons absorbed by neutral impurities [24].

(v) Similarly, the ionization or excitation probability ($f(E_A)$) of a neutral acceptor state to be ionized is given by

$$f(E_A) = 1 - \frac{1}{1 + 4e^{(E_A - E_F)/k_B T}}, \tag{4}$$

where E_A is the binding energy of a p-type impurity at its neutral state, E_F is the Fermi energy level, E_V is the energy level of the valence band in Ge, and $(E_F - E_V) = k_B T ln(N_V/N_A)$ with $N_V = 2(2\pi m^* k_B T/h^2)^{3/2}$ being the effective states, m^* is the effective mass of a hole, k_B is the Boltzmann constant [24]. However, the recoil energy produced by *pp* neutrinos could only produce a few charge carriers by exciting these impurities. Such a small signal could be immersed in the noise of the generic Ge detectors. If the charge carriers can be internally amplified to surpass the level of electronic noise, then such a small signal created by *pp* neutrinos can be detected by a GeICA detector.

3. Absorption cross section

A critical question related to the above detector working principle is the phonon absorption cross section. The scattering mechanism of phonons off the neutral impurities at low-temperature regime is governed by the following reactions

$$D^X + \Delta E_D \rightarrow e^- + D^+; A^X + \Delta E_A \rightarrow h^+ + A^-, \tag{5}$$

where D^X represents neutral donors, ΔE_D is the energy absorbed by neutral donors, e^- is the charge carrier produced after ionization of impurity. Here, ΔE_D is the energy of the incoming phonon. The absorption cross section is independent of the incoming particle but rather depends upon the incoming particle's energy (frequency). The net impurities present in our crystal for this work is 2×10^{10} cm^{-3} and the energy of phonons we have used ranges from 0.003 25 to 0.026 eV. Using a direct analogy to photons having energy $\hbar\omega$ as quanta of excitation of the lattice vibration mode of angular frequency ω, the angular frequency of phonons with energy from 0.003 25 to 0.026 eV is in the range of 4.92×10^{12}–3.94×10^{13} Hz. According to Majumdar [32], the cross section of scattering of lattice waves (phonons) off an impurity with radius R is given by

$$\sigma = \pi R^2 \chi^4/(\chi^4 + 1), \tag{6}$$

where $\chi = \omega R/v$ is called the size parameter, v is the group velocity of phonons assumed to be a constant, which is equal to the speed of sound in Ge, ω is the angular frequency of phonons. For calculating the effective radius of impurities in Ge, we have used the effective mass approximation [33] with effective Bohr's radius (R) of impurities:

$$R = 0.53\ \text{Å}\varepsilon/(m^*/m), \tag{7}$$

where ε is the dielectric constant of Ge which is equal to 16, m^* is the hydrogenic effective mass [34]. The value of m^*/m is taken to be 0.21 in the case of holes in *p*-type Ge. Using these values we have calculated the values of cross sections for various energies of phonons which are depicted in table 2. From table 2 we can infer that for the range of the phonon energies we have used in this work, the absorption cross sections are almost a constant, which is $\sim 5 \times 10^{-13}$ cm^2. Note that the estimated cross section is mainly a geometrical cross

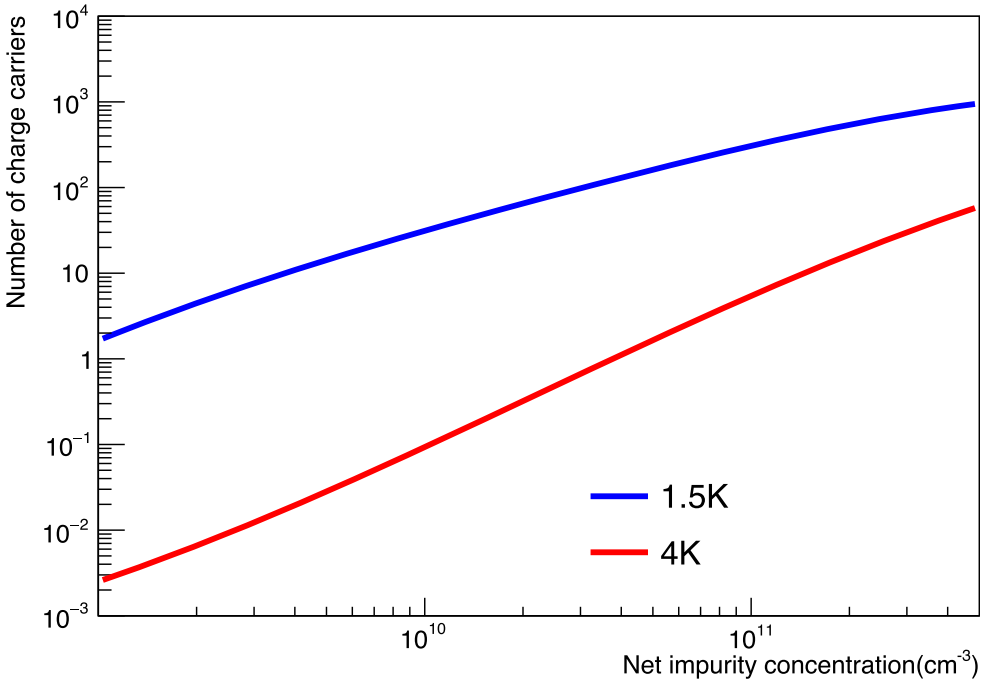

Figure 3. Number of charge carriers for different impurities in a Ge detector when the detector is operated at a very low temperatures of 1.5 K and 4 K.

section, which largely depends on the radius of the impurity. This is valid because the ionization cross section can be estimated using the electron impact ionization cross section of hydrogen atom [35] scaled by effective masses and the dielectric function.

4. Projected sensitivity

If we assume a Ge detector of 3 cm thickness with a total energy deposition of 2.0 eV, where each phonon has the energy of 0.026 eV, then the total number of parent phonons is ∼76. During the transport, each parent phonon undergoes anharmonic decay to generate two daughter phonons, each of which has energy equal to half of the parent phonon. We can estimate the total number of charge carriers N_{carriers} using the formula below:

$$N_{\text{carriers}} = \sum_i n_i p_i f(E_A)_i, \tag{8}$$

where n_i is the number of ith phonons where $i = 1, 2, 3,\ldots$ is the order of phonons which are generated in the anharmonic decay sequence and p_i is the absorption probability of ith phonons given by equation (3) and $f(E_A)_i$ is the ionization or excitation probability of ith phonons given by equation (4). Figure 3 shows the total number of charge carriers created by the ionization or excitation of impurities as a function of impurity level in a given Ge detector with an energy threshold of 2.0 eV for two temperatures, 1.5 K and 4 K.

At 1.5 K temperature, the total number of charge carriers generated in a detector with net impurity 3×10^{10} cm^{-3} is about 90 as shown in figure 3. Note that these charge carriers are created by the different generations of the daughter phonons, from the parent phonons of

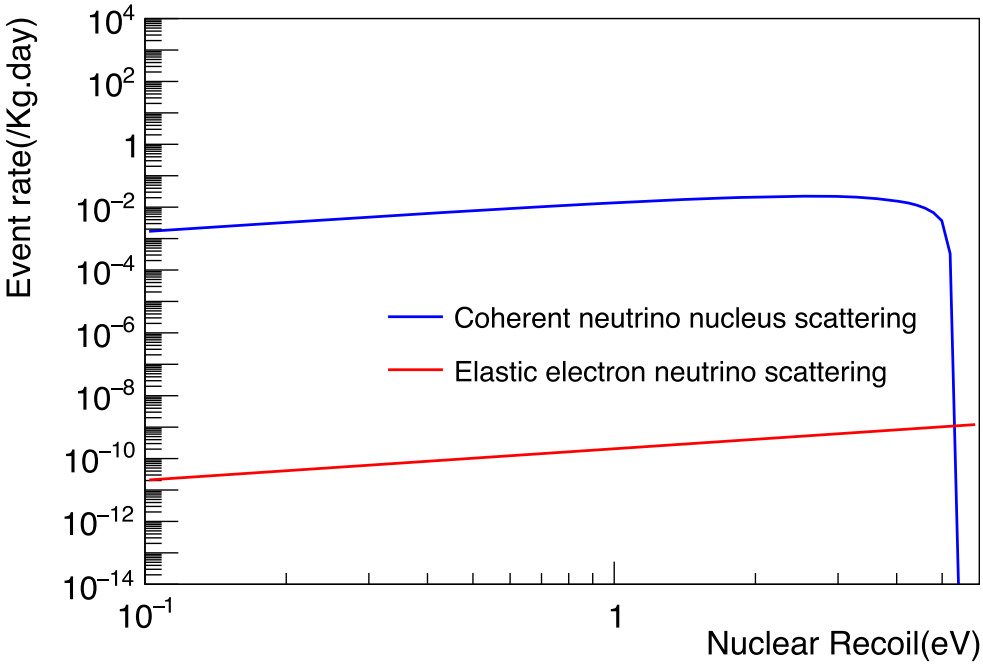

Figure 4. Event rate for pp solar neutrinos in a Ge detector of different threshold energies for elastic neutrino-electron scattering and coherent neutrino-nucleus scattering.

0.026 eV energy. With an impurity level of $7 \times 10^{10}\,\mathrm{cm}^{-3}$, at least one charge carrier can be produced when the detector is operated at 4 K.

Utilizing the flux and energy of *pp* neutrinos [1] in equation (1) and (2), we plotted the energy threshold versus the event rate for coherent neutrino-nucleus scattering (the blue curve) as shown in figure 4. Note that when neutrinos interact with electrons via the exchange of neutral Z^0 bosons, the differential cross section is given by

$$\frac{\mathrm{d}\sigma_{ES}}{\mathrm{d}T_r} = \frac{G_f^2 m_e}{2\pi}\left[(g_\nu + g_a)^2 + (g_\nu - g_a)^2\left(1 - \frac{T_r}{E_\nu}\right)^2 + (g_a^2 - g_\nu^2)\frac{m_e T_r}{E_\nu^2}\right], \tag{9}$$

where m_e is the electron mass, T_r is the electronic recoil, E_ν is the energy of incoming neutrinos, g_ν and g_a are the vector and axial couplings respectively and are defined such that

$$g_\nu = 2\sin\theta_w - \frac{1}{2},\ g_a = -\frac{1}{2}, \tag{10}$$

where $\sin^2\theta_w$ is equal to 0.223 [27]. Using the flux and energy of *pp* neutrinos [1] in equations 2 and 9, the event rate for neutrino-electron scattering versus recoil energy is shown as the red curve in figure 4. It is clear that the event rate induced by neutrino-electron scattering (the red curve) is much smaller than that of coherent neutrino-nucleus scattering (the blue curve). Therefore, coherent neutrino-nucleus scattering is studied in this work.

The event rate for *pp* neutrinos is maximized at 2.6 eV for 1 kg exposure for a year. Figure 5 shows the variation in the number of charge carriers for different detection threshold energies. We can see that at two extremely low temperatures 1.5 K and 4 K, the number of charge carriers increases as the energy increases for *pp* solar neutrinos in a Ge detector. For

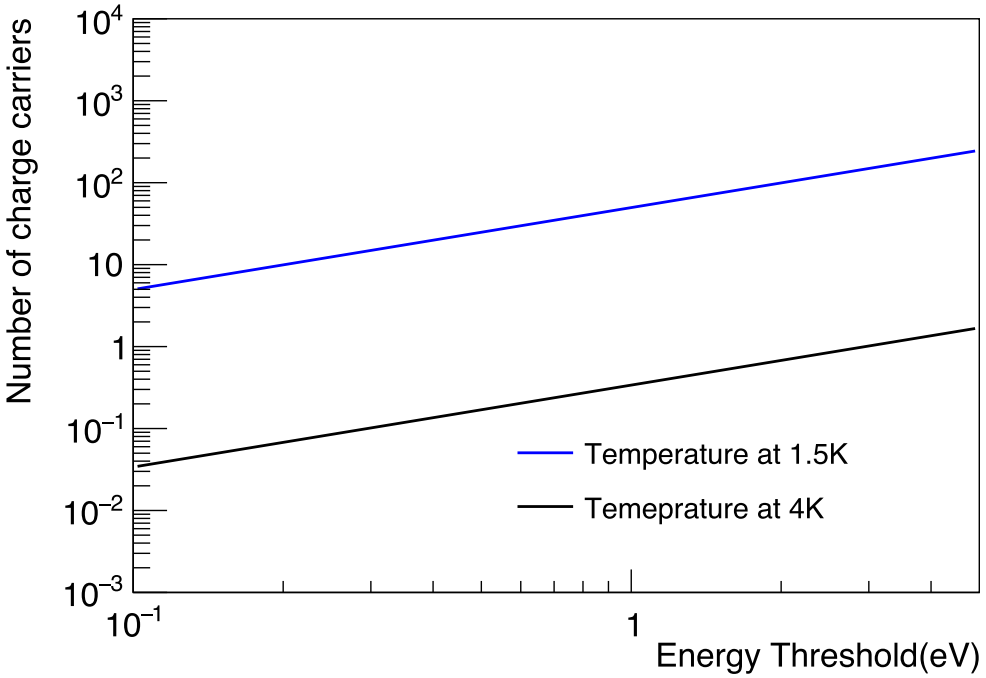

Figure 5. Number of charge carriers produced by phonons produced by pp neutrinos in a Ge detector for different threshold energies.

example, the event rate is maximum at 2.6 eV where the number of charge carriers is ∼110 at 1.5 K and ∼0.5 at 4 K. The event rate variation versus the number of charge carriers is shown in figure 6. The detector is most sensitive around 2.6 eV where the number of charge carriers is ∼110 at 1.5 K. One can expect that a 10 kg detector with an exposure of one year would obtain ∼1000 events, which is a ∼3% precision in terms of measuring the *pp* neutrino flux.

The number of charge carriers can be converted into electric current I as

$$I = n_{\text{carriers}} q/t, \tag{11}$$

where n_{carriers} is the number of the charge carriers, q is the unit of charge equal to $1.6 \times 10^{-}19$ coulombs and t is the charge collection time in the detector. If one assumes $t = 1$ microsecond, we can project the amount of current when *pp* solar neutrinos hit our detector as shown in figure 7. If the detector is capable of amplifying charge carriers by a factor of 100 through internal charge amplification, the value of the current obtained from a single charge carrier is in the order of pico amperes. Hence, this current can be collected by a detector as described by D Mei *et al* [24] which is the principle of this work. To create a single charge carrier, a phonon with an energy of 0.01 eV can excite or ionize the impurity atoms in a Ge detector. This means that the detector threshold can be as low as 0.01 eV.

Note that the background events can come from external and internal sources. Since the proposed detector is to have a threshold of 0.01 eV and the region of interest (ROI) for detecting *pp* neutrinos is between 0.1 and 5.2 eV, in such a low-energy window, we expected both external and internal background events to be negligible. This is because: (1) the external radioactive backgrounds and the muon-induced backgrounds can be minimized when the detector is operated underground with a well-shielded experimental setup [24], and (2) the radioactivity inside the detector often generates background events through the Compton

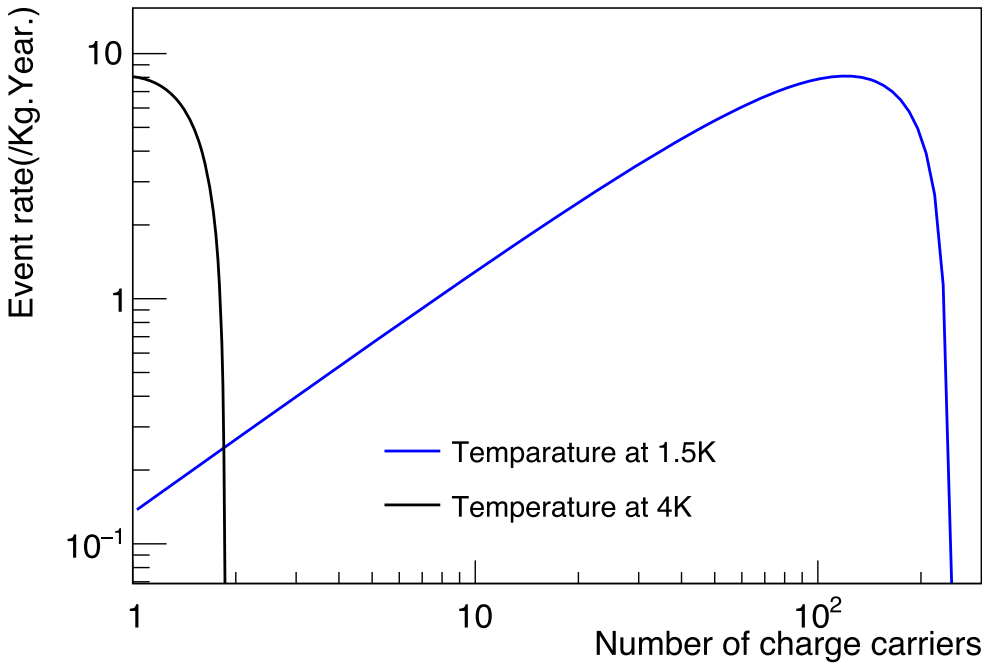

Figure 6. Event rate of pp neutrinos in a Ge detector when the detector is operated at 1.5 K and 4 K.

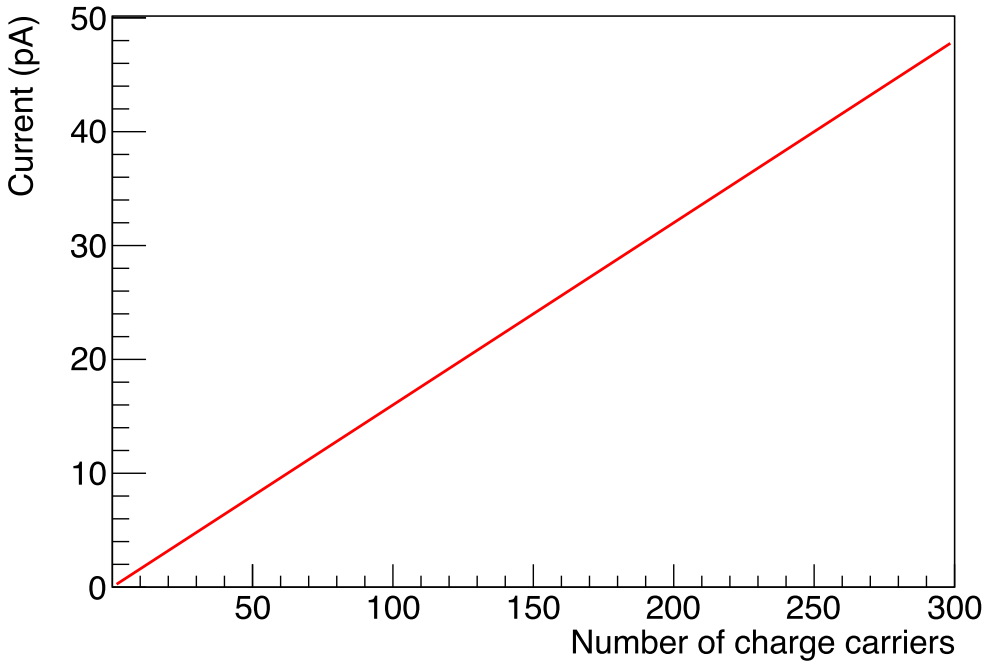

Figure 7. Current signal in the Ge detector when the pp neutrinos produce different number of charge carriers through phonon channel.

Table 1. Maximum nuclear recoil and total event rate integrated for solar neutrinos.

Type	Maximum nuclear recoil (eV)	Total event (/kg. year)
pp	5.29	16.58
pep	61.32	0.46
hep	10 386.03	0.001
$^{7}Be_{low}$	4.27	0.11
$^{7}Be_{high}$	21.87	4.98
^{8}B	6654	1.86
^{13}N	42.58	0.67
^{15}O	88.71	1.09
^{17}F	89.53	0.03

(inelastic) scattering process. These inelastic scattering of electrons by γ rays are usually in the energy region of keV, much larger than the ROI for eV-scale Ge experiments [36, 37]. The only notable and unavoidable background is due to the elastic scattering of external neutrons originating from (α, n) reactions. These neutrons can be avoided effectively by using appropriate shielding [22, 38]. A more detailed discussion about the backgrounds of this type of detector is discussed by D Mei *et al* [24]. A main source of the background events is the correlated background from other solar neutrinos. Other than the above sources of background events, for a low threshold detector, a common source of background is the various sources of noise associated with the cooling system, electronics, and cables. However, this can be usually resolved by using a good cooling system, better electronics, and cables. Therefore, we assume this can be put in control in this paper. Note that there are always possible unknown backgrounds in the region of interest in reality and they will have to be addressed in a real experiment.

It is worth mentioning that there are several sources of systematic uncertainties in the ROI for detecting *pp* neutrinos. The first is the systematic uncertainty due to the subtraction of background events in the ROI. For example, the prominent sources of the background are the other solar neutrinos such as ^{8}B and ^{7}Be, etc. The values of neutrino fluxes for all solar neutrinos used in the evaluation of the systematic uncertainty are calculated by using high metallicity SSM [1, 39]. The *pp* and *pep* neutrino fluxes are determined with $\leqslant 1\%$ accuracy. However, the uncertainty in the fluxes of other solar neutrinos varies from 6% to 30% [39]. These large uncertainties in the flux are one of the main sources of systematic uncertainty. Table 1 shows the calculated total event rates for *pp* neutrinos is 16.58 events/kg.year and the sum of the event rate of all other solar neutrinos is 9.201 events/kg.year, which are spread over a large energy range as stated in table 1. In the ROI, a total of $\sim$1.2 events/kg.year from other neutrinos are expected. Although the uncertainty of the flux can be as large as 30%, the contribution to the background reduction in the ROI is much smaller than the expected signal events. Hence, the systematic uncertainty from the background deduction is small. The second source of systematic uncertainty is the detection efficiency of a single charge carrier. The proposed detector is able to detect a single charge carrier. Due to the complexity of charge trapping, the proposed detector may lose charges, which results in a limited charge collection efficiency. However, this uncertainty should be minimized under a high field in which the charge trapping is negligible. The final uncertainty is associated with the amplification factor that amplifies a single charge carrier through internal charge amplification. The amplification factor (K) is given by $K = 2^{h/l}$ where h is the length of the avalanche region and l is the free electron path of inelastic scattering. The approximate value of l and h in a planar

Table 2. Phonon-impurity cross sections for various energies of phonons and their corresponding angular frequencies.

Honon energy (eV)	Frequency (Hz)	Effective radius (cm)	Size parameter (χ)	$\chi^4/(\chi^4+1)$	Cross section (cm^2)
0.037	5.61×10^{13}	4.03×10^{-7}	42.01	1	5.12×10^{-13}
0.026	3.94×10^{13}	4.03×10^{-7}	29.52	0.999	5.12×10^{-13}
0.013	1.51×10^{13}	4.03×10^{-7}	11.35	0.999	5.11×10^{-13}
0.0065	9.87×10^{12}	4.03×10^{-7}	7.38	0.999	5.11×10^{-13}
0.003 25	4.93×10^{12}	4.03×10^{-7}	3.69	0.994	5.09×10^{-13}

Ge detector of 3cm thickness at 4 K is about 0.5 μm and 5 μm respectively. This leads to an amplification factor of about 1000 [24]. However, the value of K is governed by the electric field, the concentration of impurities, and the gradient of temperature in the detector. Due to the uncertainties in these parameters, it is difficult to obtain a constant value of K. The spread of the K value is likely to impact the stability of the detection threshold and hence causes systematic uncertainty in detecting *pp* neutrinos. In summary, there will be some system uncertainties in detecting *pp* neutrinos using the proposed low-threshold detector. When designing a detector system, those systematic uncertainties should be minimized to be less than the statistical error.

5. Conclusion

We present a viable detection method for studying *pp* neutrinos using coherent elastic neutrino-nucleus scattering in a novel Ge detector with internal charge amplification. The very low energy deposition of *pp* neutrinos interacting with Ge nucleus is dissipated through the emission of phonons. The diffusion of those phonons will undergo anharmonic decay. It is the propagation of those phonons that will excite and ionize impurities in Ge, which will allow us to detect the energy deposition from *pp* neutrinos as low as 0.01 eV. If a Ge detector can internally amplify the charge signal by a factor of 100, then the charge carriers of $\sim$100 can be detected with a current of $\sim$1 pA, which is a normal signal from a Ge detector.

Acknowledgments

The authors would like to thank Christina Keller for their careful reading of this manuscript. This work was supported by NSF OISE-1743790, DOE FG02-10ER46709, DE-SC0004768, the Office of Research at the University of South Dakota, and a research center supported by the State of South Dakota.

Data availability statement

All data that support the findings of this study are included within the article (and any supplementary files).

ORCID iDs

D-M Mei https://orcid.org/0000-0002-2881-4706

References

[1] Papoulias D K, Sahu R, Kosmas T S, Kota V K B and Nayak B 2018 Novel neutrino-floor and dark matter searches with deformed shell model calculations *Adv. High Energy Phys.* **2018** 6031362
[2] Bahcall J N, Basu S and Pinsonneault M H 1998 How uncertain are solar neutrino predictions? *Phys. Lett.* B **433** 1–8
[3] Brun A S, Turck-Chieze S and Morel P 1998 Standard solar models in the light of new helioseismic constraints. I. the solar core *Astrophys. J.* **506** 913
[4] Davis R 1994 A review of the homestake solar neutrino experiment *Prog. Part. Nucl. Phys.* **32** 13
[5] Fukuda S *et al* 2001 Solar ^{8}b and hep neutrino measurements from 1258 d of Super-Kamiokande data *Phys. Rev. Lett.* **86** 5651
[6] Suzuki Y 2019 The Super-Kamiokande experiment *Eur. Phys. J.* C **79** 1–18
[7] Harrison P F, Perkins D H and Scott W G 2002 Tri-bimaximal mixing and the neutrino oscillation data *Phys. Lett.* B **530** 167–73
[8] Aharmim B *et al* 2019 Constraints on neutrino lifetime from the sudbury neutrino observatory *Phys. Rev.* D **99** 032013
[9] Arpesella C *et al* 2008 Direct measurement of the ^{7}be solar neutrino flux with 192 d of borexino data *Phys. Rev. Lett.* **101** 091302
[10] Kumaran S, Ludhova L, Penek Ö and Settanta G 2021 Borexino results on neutrinos from the Sun and Earth *Universe* **7** 231
[11] Altmann M *et al* 2005 Complete results for five years of GNO solar neutrino observations *Phys. Lett.* B **616** 174–90
[12] Abdurashitov J N *et al* 1994 Results from SAGE (the Russian-American gallium solar neutrino experiment) *Phys. Lett.* B **328** 234–48
[13] Cribier M *et al* 2000 The lens experiment *Nucl. Phys. B* **87** 195–7
[14] Guenther D B, Demarque P, Kim Y C and Pinsonneault M H 1992 Standard solar model *Astrophys. J.* **387** 372–93
[15] Agostini M *et al* 2018 Comprehensive measurement of pp-chain solar neutrinos *Nature* **562** 505–10
[16] Wolfenstein L 1978 Neutrino oscillations in matter *Phys. Rev.* D **17** 2369
[17] Wolfenstein L 1979 Neutrino oscillations and stellar collapse *Phys. Rev.* D **20** 2634
[18] Bahcall J N, Serenelli A M and Basu S 2006 10,000 standard solar models: a Monte Carlo simulation *Astrophys. J. Suppl. Ser.* **165** 400
[19] Esteban I, Gonzalez-Garcia M C, Maltoni M, Martinez-Soler I and Schwetz T 2017 Updated fit to three neutrino mixing: exploring the accelerator-reactor complementarity *J. High Energy Phys.* **JHEP17(2017)87**
[20] Z Ahmed (CDMS collaboration) *et al* 2009 Search for weakly interacting massive particles with the first five-tower data from the cryogenic dark matter search at the Soudan Underground Laboratory *Phys. Rev. Lett.* **102** 011301
[21] Agnese R *et al* 2014 Search for low-mass weakly interacting massive particles with SuperCDMS *Phys. Rev. Lett.* **112** 241302
[22] Armengaud E *et al* 2013 Background studies for the EDELWEISS dark matter experiment *Astropart. Phys.* **47** 1–9
[23] Agnese R *et al* 2018 First dark matter constraints from a SuperCDMS single-charge sensitive detector *Phys. Rev. Lett.* **121** 051301
[24] Mei D, Wang G, Mei H, Yang G, Liu J, Wagner M, Panth R, Kooi K, Yang Y and Wei W 2018 Direct detection of MeV-scale dark matter utilizing germanium internal amplification for the charge created by the ionization of impurities *Eur. Phys. J.* C **78** 187
[25] Bhattarai S, Mei D and Raut M S 2020 Low-energy solar neutrino detection utilizing advanced germanium detectors *APS Meeting Abstracts* **vol 2020** SF.002
[26] Starostin A S and Beda A G 2000 Germanium detector with an internal amplification for investigating rare processes *Phys. At. Nucl.* **63** 1297–300

[27] Billard J, Strigari L E and Figueroa-Feliciano E 2015 Solar neutrino physics with low-threshold dark matter detectors *Phys. Rev.* D **91** 095023
[28] Yang G, Govani J, Mei H, Guan Y, Wang G, Huang M and Mei D 2014 Investigation of influential factors on the purification of zone-refined germanium ingot *Cryst. Res. Technol.* **49** 269–75
[29] Czochralski J 1918 Ein neues verfahren zur messung der kristallisationsgeschwindigkeit der metalle *Z. Phys. Chem.* **92** 219–21
[30] Wang G, Sun Y, Yang G, Xiang W, Guan Y, Mei D, Keller C and Chan Y 2012 Development of large size high-purity germanium crystal growth *J. Cryst. Growth* **352** 27–30
[31] Wittmann R 2007 Miniaturization problems in CMOS technology: investigation of doping profiles and reliability *Ph. D. Thesis* Vienna University of Technology
[32] ASME Majumdar. Microscale heat conduction in dielectric thin films. 1993.
[33] Skinner B 2019 Properties of the donor impurity band in mixed valence insulators *Phys. Rev. Mater.* **3** 104601
[34] Dubon O D Jr. 1996 *Electronic Processes in Uniaxially Stressed P-Type Germanium* (Berkeley, CA: University of California)
[35] Percival I C 1966 Cross sections for collisions of electrons with hydrogen atoms and hydrogen-like ions *Nucl. Fusion* **6** 182
[36] Alexander J *et al* 2016 Dark sectors 2016 workshop: community report arXiv:1608.08632
[37] Kane P P 1992 Inelastic scattering of x-rays and gamma rays by inner shell electrons *Phys. Rep.* **218** 67–139
[38] Agnese R *et al* 2017 Projected sensitivity of the SuperCDMS SNOLAB experiment *Phys. Rev.* D **95** 082002
[39] Villante F L and Serenelli A 2020 The relevance of nuclear reactions for standard solar models construction *Front. Astron. Space Sci.* **7** 112